

Thermal Expansion, Electrical Resistivity, and Spreading Area of Sn-Zn-In Alloys

Tomasz Gancarz, Przemysław Fima, and Janusz Pstruś

(Submitted August 22, 2013; in revised form December 3, 2013; published online December 18, 2013)

Thermal expansion and electrical resistivity of alloys based on Sn-Zn eutectic with 0.5, 1.0, 1.5, and 4.0 wt.% additions of In were studied. Thermal expansion measurements were performed using thermo-mechanical analysis tester over 223–373 K temperature range. Electrical resistivity measurements were performed with four-probe method over 298–423 K temperature range. The electrical resistivity of alloys increases linearly with temperature and concentration of In; also coefficient of thermal expansion of the studied alloys increases with In concentration. Scanning electron microscopy revealed simple eutectic microstructure with In dissolved in Sn-rich matrix. The results obtained were compared with the available literature data. Spreading tests on Cu of Sn-8.8Zn alloys with 0.5, 1.0, and 1.5 at.% of In were performed. Wetting tests were performed at 250 °C, by sessile drop method, by means of flux, and wetting times were 3, 8, 15, 30, and 60 min. In general, no clear effect of wetting time on spreading was observed.

Keywords electrical resistivity, microstructure, Sn-Zn-In alloys, thermal expansion

1. Introduction

Worldwide studies on Pb-free replacement for traditional solders lead to two groups of alloys that can be used commercially. One of them constitutes the alloys of the Sn-Ag-Cu system (Ref 1), whereas the other constitutes the alloys based on Sn-Zn eutectic (Ref 2, 3). The great advantage of Sn-Zn eutectic alloy is that its melting temperature (471 K) is close to the melting temperature of Sn-Pb eutectic solder (456 K). Low price per mass unit of Sn-Zn solder is also a favorable factor. There are some drawbacks of Sn-Zn alloys, such as relatively poor wetting compared with other lead-free solders as well as easy oxidation (Ref 3). Ternary Sn-Zn-In alloys were proposed (Ref 4) as replacement to traditional Sn-Pb solder, characterized by low melting point (348–353 K), and at the same time, improved wetting characteristics. We have shown recently (Ref 5) that wetting of Sn-Zn alloys on Cu and Ni substrates can be slightly improved by alloying it with small (0.5–1.5 wt.%) additions of indium. Thermal expansion and electrical resistivity of solders are interesting both from academic and practical points of view.

This article is an invited submission to *JMEP* selected from presentations at the Symposia “Wetting,” “Interface Design,” and “Joining Technologies” belonging to the Topic “Joining and Interface Design” at the European Congress and Exhibition on Advanced Materials and Processes (EUROMAT 2013), held September 8–13, 2013, in Sevilla, Spain, and has been expanded from the original presentation.

Tomasz Gancarz, Przemysław Fima, and Janusz Pstruś, Institute of Metallurgy and Materials Science, Polish Academy of Sciences, ul. Reymonta 25, 30-059 Krakow, Poland. Contact e-mails: tomasz.gancarz@imim.pl and t.gancarz@imim.pl.

Knowledge of thermal expansion of solders is important as large differences in coefficients of thermal expansion (CTEs) between solder and soldered parts may lead to internal tensions and resulting cracks during thermal fatigue of joints (Ref 6). Thermomechanical analysis (TMA) is one of the techniques that can be used for thermal expansion measurements (Ref 7). Electrical resistivity can be used for studying phase transitions with changes of temperature in alloys (Ref 8). Electrical resistivity depends on solder composition and varies in temperature. Four-point probe technique is the most common one that is used to study electrical resistivity of materials (Ref 8, 9), because of its relative simplicity and high accuracy. In this method, a current flow through two probes and voltage drop between the other two probes are measured.

Temperature dependence of electrical resistivity of solid Sn-Zn alloys was studied by few groups of authors. Ari et al. (Ref 10) performed measurements for two compositions (1 and 8.9 wt.% Zn), while Matsugi et al. (Ref 11) studied five compositions (1, 9, 20, 50, and 80 wt.% Zn). Both the author groups found that electrical resistivity of alloys increases monotonously with the increasing temperature. Also, at constant temperature, electrical resistivity decreases with the increasing concentration of Zn. In the case of Sn-Zn-In alloys up to 2 wt.% of In, Shalaby (Ref 12) determined the electrical resistivity at room temperature. According to the literature survey, no published data exist regarding electrical resistivity dependence on temperature and thermal expansion of Sn-Zn-In alloys, as well as thermal expansion data for Sn-Zn alloys. Therefore, the aim of this investigation is to study the effect of small additions of indium (up to 4.0 wt.%) on thermal expansion and electric resistivity dependence on temperature of Sn-Zn eutectic-based alloys.

2. Experimental

Sn-8.8Zn (eutectic) and four solders based on it containing small additions of indium: 0.5, 1.0, 1.5, and 4.0 wt.%,

respectively, were used for a study of thermal expansion and electrical resistivity. Solders were prepared by melting accurately weighted amounts of pure metals (99.999%) in graphite crucibles, under Ar (99.9992%) protective atmosphere to avoid oxidation. FEI E-SEM XL30 system was used for microstructural characterization of bulk alloys containing 1.5 and 4% of In. Energy dispersive spectroscopy (EDS) analysis was performed at 20 kV and working distance of 10 mm, by means of the standardless Analysis EDAX System based on Genesis 2000 software. In order to prepare samples for electrical resistivity measurements, the liquid alloys were sucked into quartz capillaries of 2-mm uniform inner diameter, in which they solidified rapidly. After solidification of the obtained rods, quartz capillaries were carefully removed, and the samples visually inspected. The measurements were performed with the setup described in Ref 13. The electrical resistivity ρ is determined by charging the current I through the outer probes and measuring the voltage drop U between the inner probes, which are placed at a given distance L . In the present study, L was 150 mm for all of the samples. High-quality Keithley 6220 current source (output 100 mA with an accuracy of 10 μ A) coupled with nano-voltmeter Keithley 2182 (10 mV range with an accuracy of 1 nV) connected together in DELTA mode were used in measurements. In this mode, the current source and nano-voltmeter act as a single instrument for trouble-free operation. The temperature was controlled via a high-class Eurotherm temperature controller (accuracy of 0.1 K).

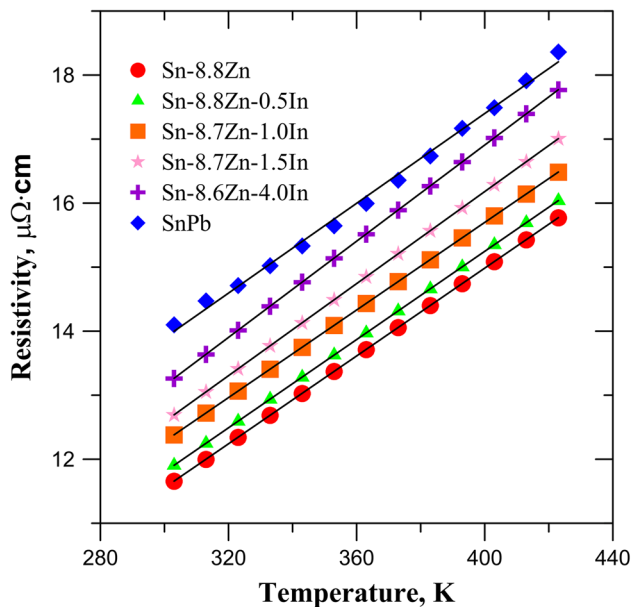


Fig. 1 Electrical resistivity of Sn-Zn-In alloys vs. temperature

Table 1 Electrical resistivity dependence on temperature, electrical resistivity at 298 K, and CTE over 223-373 K temperature range

Alloy, wt. %	$\rho = A + B \cdot T$, $\mu\Omega/\text{cm}$	ρ (298 K), $\mu\Omega/\text{cm}$	CTE, 10^{-6} K^{-1} (223-373 K)
Sn-8.8Zn	$\rho = 1.267 + 0.0342 \times T$	11.7 ± 0.1	20.88 ± 0.14
Sn-8.8Zn-0.5In	$\rho = 1.465 + 0.0344 \times T$	11.9 ± 0.1	21.05 ± 0.15
Sn-8.7Zn-1.0In	$\rho = 2.017 + 0.0342 \times T$	12.3 ± 0.1	21.32 ± 0.18
Sn-8.7Zn-1.5In	$\rho = 1.802 + 0.0359 \times T$	12.7 ± 0.1	22.17 ± 0.15
Sn-8.5Zn-4.0In	$\rho = 1.882 + 0.0375 \times T$	13.3 ± 0.1	22.37 ± 0.19
Sn-37Pb	$\rho = 3.374 + 0.0350 \times T$	14.1 ± 0.1	24.61 ± 0.19

Electrical resistance measurements were performed in the temperature range of 298-423 K. The electrical resistivity was calculated according to Eq 1:

$$\rho = \frac{U}{I} \cdot \frac{1}{L} \cdot \frac{\pi d^2}{4} \quad (\mu\Omega/\text{cm}), \quad (\text{Eq 1})$$

where ρ is the electrical resistivity, U is the voltage, I is the current, L is the distance between voltage probes, and d is the diameter of a sample. Measurements were conducted for each temperature by holding for 3 h to obtain complete stability of electrical resistivity; after cooling and heating again, the obtained values were almost identical (0.5% difference).

Thermal expansion measurements were carried out on TMA Netzsch Pegasus F1 tester, under the following experimental conditions: range of temperature: 223-373 K, heating rate: 2 K/min, gas flow: 20 mL/min, force exerted on a sample: 0.1 mN, inert protective gas: He. Samples of 5 mm in diameter and 20 mm long were used in TMA measurements. Resolution of measurement as declared by TMA tester was 0.01 μ m. Samples were mounted in the tester vertically pressed for holder. This way of mounting, as schematically shown by Lau and Chang (Ref 7), means that the TMA tester works as classical dilatometer. CTE is calculated from TMA data according to Eq 2:

$$\text{CTE} = \frac{1}{L} \frac{dL}{dT} \quad (\text{K}^{-1}), \quad (\text{Eq 2})$$

where L is the linear dimension (e.g., length), and dL/dT is the rate of change of that linear dimension per unit change in temperature.

Spreading tests on Cu substrate of Sn-8.8Zn alloys with 0.5, 1.0, and 1.5 at.% of In were performed using sessile drop (SD) method (Ref 5). Wetting tests were performed at 523 K, by means of flux (ALU33[®] components of which are aminoethylethanolamine ($\text{C}_4\text{H}_{12}\text{N}_2\text{O}$) and ammonium fluoroborate (NH_4BF_4)); the mass of the solder samples used for wetting test was 0.5 g; and the wetting times were 3, 8, 15, 30, and 60 min. After wetting tests, the flux residue was washed out with tap water. The area of spreading was calculated using the application GetArea CorelDraw12. Selected solidified solder/substrate couples were cut perpendicular to the plane of the interface, and polished for microstructural characterization. The microstructural and EDS analyses were performed using FEI Quanta 3D FEG system, at 20 kV and WD 10 mm, by means of the standard less Analysis EDAX Pegasus XM4i software.

3. Results and Discussion

The results of electrical resistivity measurements of Sn-Zn and Sn-Zn-In alloys are plotted versus temperature, and shown

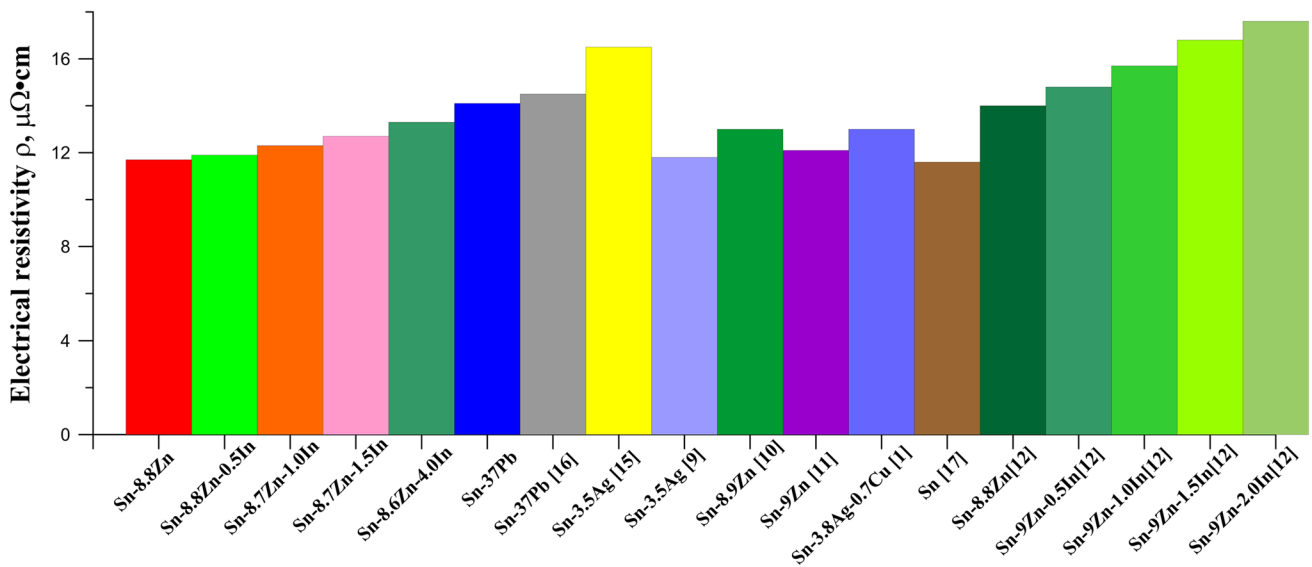


Fig. 2 Electrical resistivity of Sn-Zn-In alloys at 298 K compared with the literature data

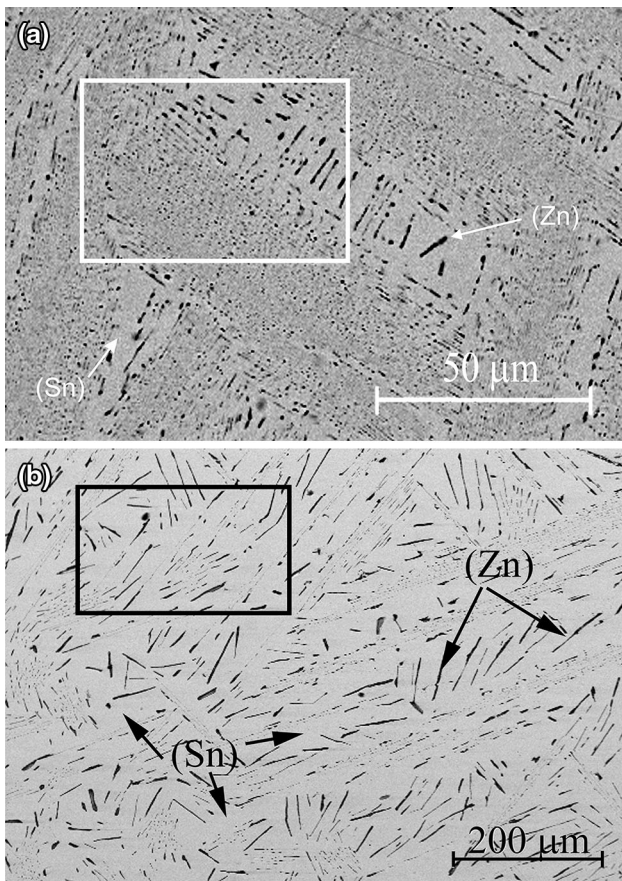


Fig. 3 SEM micrographs of alloys: (a) Sn-8.7Zn-1.5In and (b) Sn-8.6Zn-4.0In

in Fig. 1. One can see that for all the compositions studied, electrical resistivity increases monotonously with the increasing temperature, and at constant temperature, the electrical resistivity increases with the increasing concentration of indium. For comparison purposes, the results for Sn-37Pb (wt.%) alloy

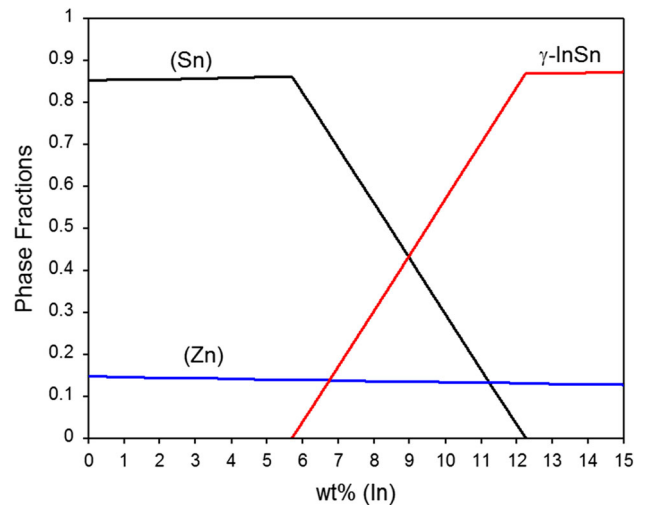


Fig. 4 Phase fractions vs. concentration of In in Sn-Zn-In alloys, as per calculations based on thermodynamic data (Ref 23) at temperature 303 K

obtained on the same setup are plotted in Fig. 1. Over the temperature range, the electrical resistivity of Sn-Zn-In alloy containing 4.0 wt.% In is about 6% lower than that of Sn-37Pb alloy. The lowest value of electrical resistivity was obtained for Sn-8.8Zn alloy—17% lower than the electrical resistivity of Sn-37Pb alloy. Our results for Sn-Zn-In alloys are close to that of 10-15 $\mu\Omega/\text{cm}$ reported (Ref 14) for SAC alloys commonly used as lead-free solders. The data presented in Fig. 1 were analyzed with the least square method, and the regressed linear equations describing electrical resistivity dependence on temperature are compiled in Table 1.

Figure 2 shows the current study's results together with the literature data for Sn3.5Ag (Ref 9, 15), Sn8.9Zn (Ref 10), Sn9Zn (Ref 11), Sn-37Pb (Ref 16), Sn-3.8Ag-0.7Cu (Ref 1) alloys, and tin (Ref 17). It is clear that the value of 11.7 $\mu\Omega/\text{cm}$ obtained in the current study for Sn8.8Zn alloy is close to 13 and 12.1 $\mu\Omega/\text{cm}$ reported for Sn8.9Zn (Ref 10) and Sn9Zn

(Ref 11) alloys, respectively. Also, very good agreement is seen in the case of Sn-37Pb alloy. The current study's results of electrical resistivity for SnZn eutectic, however, are lower than the data obtained by Shalaby (14, 14.8, 15.7, 16.8, and 17.6 $\mu\Omega/\text{cm}$) (Ref 12) for SnZn and SnZn with addition of In ranging from 0.5 to 2%, respectively. A similar difference can be observed for Sn-Zn-In alloys (Ref 12). Although it is not clear why Shalaby's data are higher, the same dependence on composition is observed, i.e., with the increasing concentration of In in Sn-Zn alloys, the electrical resistivity increases at constant temperature.

In general, regardless of differences between various sources, at 298 K, electrical resistivity of pure Sn (11.5-14 $\mu\Omega/\text{cm}$) (Ref

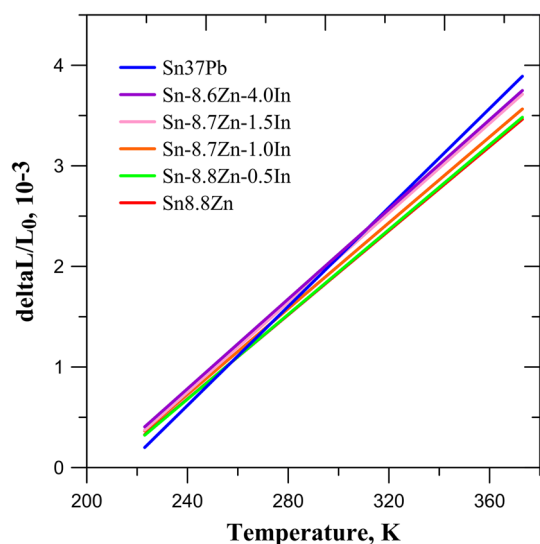


Fig. 5 Thermal expansion of Sn-Zn-In alloys vs. temperature. The order of lines in the legend corresponds to the order of lines in the upper right corner

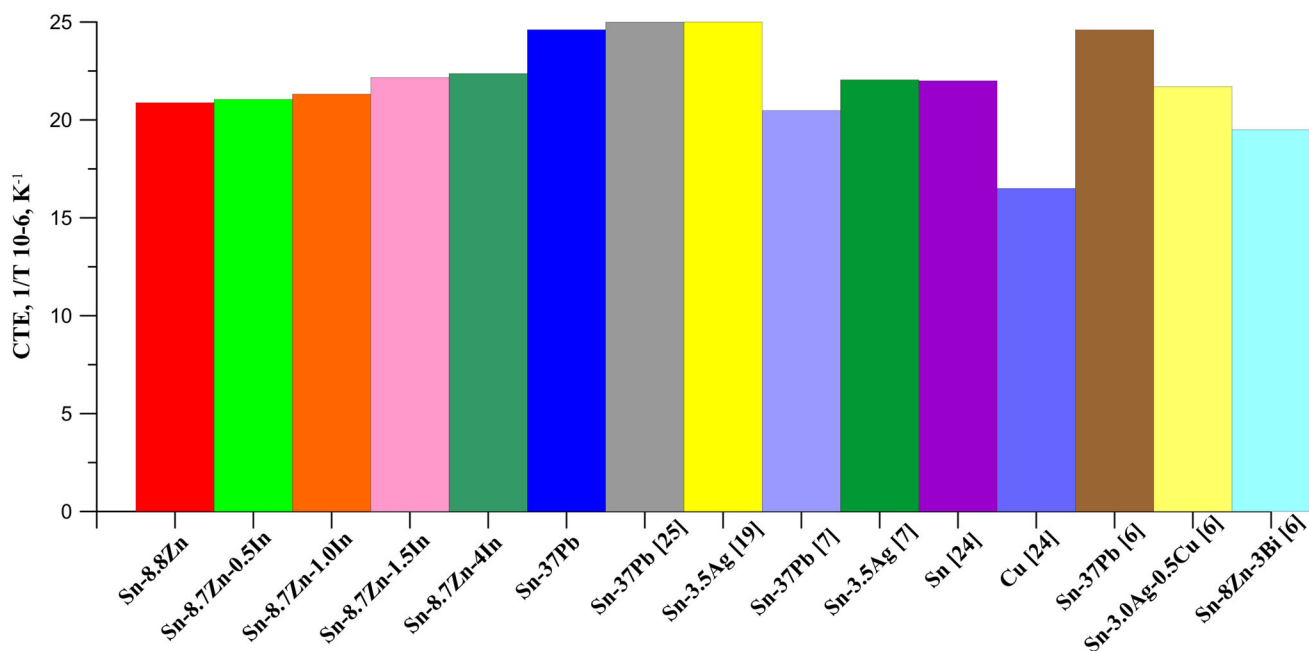


Fig. 6 Coefficient of thermal expansion (CTE) of Sn-Zn-In alloys compared with the literature data

11, 16, 17) is higher than the electrical resistivity of pure Zn (5-8 $\mu\Omega/\text{cm}$) (Ref 11, 16). For this reason, one could assume that the electrical resistivity should decrease with the increasing concentration of the component of lower resistivity, as was shown by Matsugi et al. (Ref 11). This does not always need to be true for metallic systems, especially multicomponent alloys, as an alloy composition determines its microstructure, which in turn correlates with properties including mechanical (Ref 18) and thermal (Ref 19). Figure 3 illustrates the microstructure of (a) Sn-8.7Zn-1.5In and (b) Sn-8.5Zn-4.0In alloys, respectively. In both cases, this is a simple eutectic microstructure consisting of light Sn-rich matrix (Sn) with In dissolved in it; and fine, dark Zn-rich (Zn) precipitates. Rectangles imposed on figures (a) and (b) mark the limits of alloy subjected to EDS analysis, results of which are (a) Sn-8.0Zn-2.9In, and (b) Sn-7.2Zn-4.5In, respectively. This microstructure resembles those of near-eutectic Sn-Zn alloys (Ref 20-22). According to phase diagram of Sn-Zn-In system assessed by Cui et al. (Ref 23), addition of up to 5 wt.% of In to Sn-8.8Zn eutectic does not affect its microstructure. As can be seen in Fig. 4, as per calculations based on thermodynamic data of Cui et al. (Ref 23) at temperature 303 K, below 5 wt.% of In, there are two phases present, i.e., (Sn) and (Zn), and their proportions do not significantly change with the increasing concentration of indium. Above 5.5 wt.% of In, low melting γ -InSn phase appears, which limits possible application of those alloys. The increase of electrical resistivity with the indium concentration is not a result of changes of eutectic microstructure of the studied alloys but only a result of concentration, even though electrical resistivity of In (8 and 8.4 $\mu\Omega/\text{cm}$) (Ref 16, 24) is lower than the electrical resistivity of Sn-8.8Zn eutectic alloy.

The alloys studied in this investigation expand linearly over the 223-373 K temperature range, as can be seen in Fig. 5. Often-quoted CTE of copper is $17.1 \times 10^{-6} \text{ K}^{-1}$ at 293-573 K range (Ref 24) and 17.7 K^{-1} (Ref 16). For better solder joint thermal-fatigue reliability, it is preferable to have CTE of solder close to soldered materials. The CTEs of Sn-Zn-In alloys

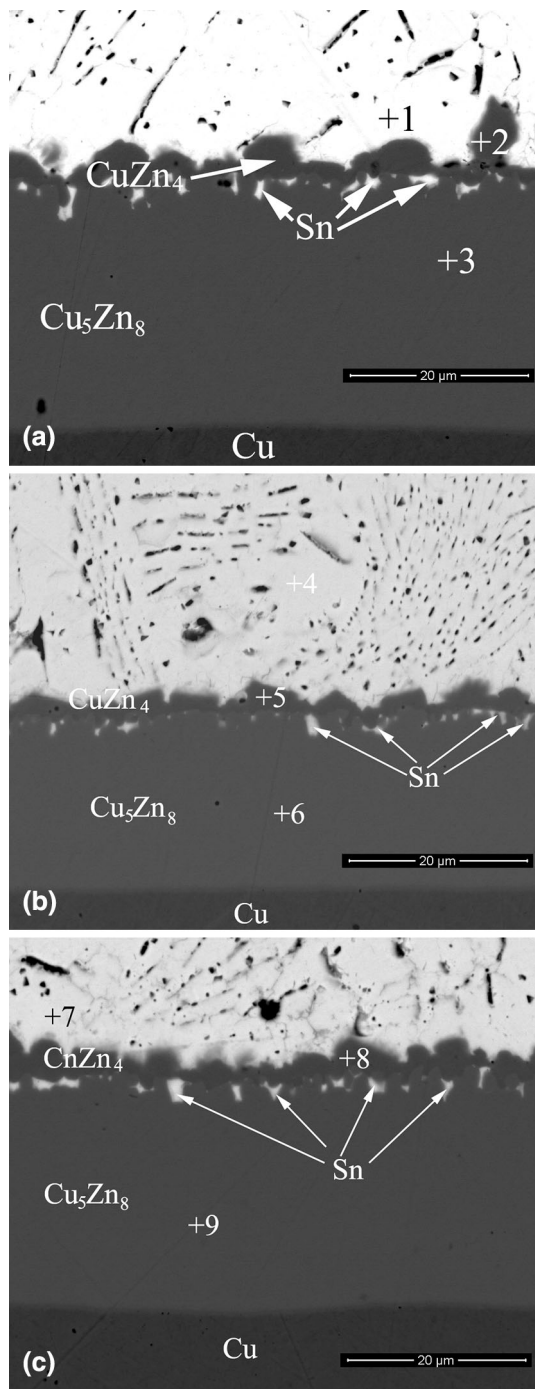


Fig. 7 Microstructures of cross sections of the Sn-Zn-In solder/Cu substrate interface after 60 min at 523 K: (a) 0.5, (b) 1.0, and (c) 1.5 at.% of In, respectively

(21.05, 21.32, 22.17, and $22.37 \times 10^{-6} \text{ K}^{-1}$ for 0.5, 1.0, 1.5, and 4.0 wt.% In, respectively) are slightly higher than that of Sn-8.8Zn ($20.88 \times 10^{-6} \text{ K}^{-1}$) and lower than that of Sn-37Pb ($24.61 \times 10^{-6} \text{ K}^{-1}$) alloys determined in present study. One could see very good agreement of the present CTE for Sn-37Pb alloy with the reference data (Ref 25). The same situation can be observed when we compare our own data with the data presented for Sn-37Pb $20.48 \times 10^{-6} \text{ K}^{-1}$ (Ref 7). In general, there are sometimes large differences (see Fig. 6) in the reported CTE data for the same alloy systems. For example, the

Table 2 EDS analysis results at the points indicated in Fig. 7

Point	Elements in at.%			
	Cu	Zn	Sn	In
1		6.88	91.92	1.2
2	20.19	79.81		
3	34.14	65.86		
4		6.58	91.56	1.86
5	20.1	79.9		
6	34.33	65.67		
7		6.53	91.25	2.22
8	20.18	79.82		
9	34.51	65.49		

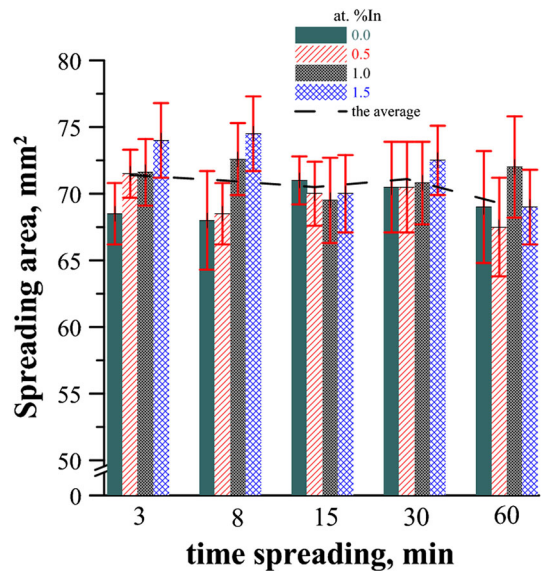


Fig. 8 Effects of In concentration and time on spreading area of Sn-Zn-xIn alloys ($x = 0.5, 1, \text{ and } 1.5$)

CTE of Sn-37Pb alloy reported by Ref 7 is 16.8% lower than that of Ref 6. Since there are no literature data on CTE of Sn-Zn-In alloys, we cannot compare our results directly. However, our results indicate that CTE of Sn-Zn-In alloys is lower than that of Sn-37Pb alloy or that of Pb-free alternatives, such as Sn-3.8Ag-0.7Cu (Ref 6), which means that it can be a better choice for joints with copper, which are subjected to thermal cycling. Contrary to electrical resistivity, the increase of the CTE of Sn-Zn-In alloys with the increasing concentration of In can be attributed to the higher CTE of In ($32.1 \times 10^{-6} \text{ K}^{-1}$ (Ref 24)) compared with Sn-8.8Zn eutectic.

Figure 7 presents the examples of microstructure of cross-sectioned solder/Cu substrate interface after spreading tests for 60 min at 250 °C. One can see on the interface, the products of reaction between liquid solders with Cu substrate, i.e., intermetallic phases CuZn_4 and Cu_5Zn_8 , which fact was also confirmed by EDS measurement (Table 2). The thickness of Cu_5Zn_8 (bottom) is noticeably larger than that of CuZn_4 (top); also, light areas of pure Sn are observed between the intermetallics layers, which is in agreement with the literature data (Ref 5) (although in Ref 5, no analysis of upper layer and light areas between the layers was provided). Spreading test results shown in Fig. 8 present spreading areas of Sn-8.8Zn

alloys with 0.5, 1.0, and 1.5 at.% of In on Cu substrate. There is no clear trend in the changes of spreading area due to the effect of indium addition to eutectic Sn-Zn or due to the increase in the time of spreading test up to 60 min.

4. Conclusion

Thermoelectric properties of alloys based on Sn-Zn eutectic with 0.5, 1.0, 1.5, and 4.0 wt.% In additions were studied with the increasing temperature. Four-point probe technique was applied to study electrical resistivity, and TMA was applied to determine CTE. Study of microstructures of Sn-Zn-In alloys revealed that In does not affect eutectic microstructure of Sn-8.8Zn solder, which is in agreement with the literature data. The electrical resistivity of alloys increases with the temperature and concentration of In; also, CTE increases with In concentration. The increase of CTE with the increasing In concentration can be attributed to the fact that CTE of In is higher than the respective data for Sn-8.8Zn eutectic alloy. Properties of alloys based on Sn8.8Zn eutectic with In additions of 0.5, 1.0, 1.5, and 4.0 wt.% are more favorable (lower electrical resistivity and CTE) compared with the traditional Sn-37Pb solder. In general, no clear effects of wetting time and addition of In to alloys on spreading were observed.

Acknowledgments

This study was financed under the framework of the project POIG.01.01.02-00-015/09, co-funded by the European Regional Development Fund (ERDF) and the Government of Poland under the Innovative Economy Program.

Open Access

This article is distributed under the terms of the Creative Commons Attribution License which permits any use, distribution, and reproduction in any medium, provided the original author(s) and the source are credited.

References

1. C. Schmetterer, A. Mikula, and H. Ipsner, *Database for Properties of Lead-Free Solder Alloys*, 2006, www.syncpower.com/datasheet/db_pbfree_solder.pdf. Accessed 20 August, 2013
2. K. Suganuma and K.S. Kim, Sn-Zn Low Temperature Solder, *J. Mater. Sci.: Mater. Electron.*, 2007, **18**, p 121–127
3. L. Zhang, S. Xue, L. Gao, Z. Sheng, and H. Ye, Development of Sn-Zn Lead-Free Solders Bearing Alloying Elements, *J. Mater. Sci.: Mater. Electron.*, 2010, **21**, p 1–15
4. M. McCormack, S. Jin, and H.S. Chen, New Lead-Free Sn-Zn-In Solder Alloys, *J. Electron. Mater.*, 1994, **23**, p 687–690
5. P. Fima, T. Gancarz, J. Pstrus, and A. Sypien, Wetting of Sn-Zn-xIn ($x = 0.5, 1.0, 1.5$ wt%) Alloys on Cu and Ni Substrates, *J. Mater. Eng. Perform.*, 2012, **21**, p 595–598
6. Y. Nakagawa, Y. Aoki, and T. Nagai, *Evaluating Joint Reliability of Sn-Zn Low-Temperature, Lead-Free Solder*, Espec Environmental Test Technology Center Corp., Yokohama Branch http://www.espec.co.jp/english/tech-info/tech_info/tech-report_pdf_a08.html. Accessed 20 August, 2013
7. J. Lau and C. Chang, TMA, DMA, DSC and TGA of Lead Free Solders, *Solder. Surf. Mt. Technol.*, 1999, **11**, p 17–24
8. E. Cadirli, H. Kaya, A. Gumus, and I. Yilmazer, Temperature Dependence of Electrical Resistivity of Cd-Sn, Bi-Sn, and Al-Si Eutectic, and Al-3wt%Si Hypoeutectic Alloys, *J. Mater. Eng. Perform.*, 2006, **15**, p 490–493
9. R. Kisiel, W. Gasior, Z. Moser, J. Pstrus, K. Bukat, and J. Sitek (Sn-Ag)eut + Cu Soldering Materials Part II: Electrical and Mechanical Studies, *J. Phase Equilibria Diffusion*, 2004, **25**, p 122–124
10. M. Ari, B. Saatçi, M. Gündüz, M. Payveren, and S. Durmuş, Thermo-Electrical Characterization of Sn-Zn Alloys, *Mater. Charact.*, 2008, **59**, p 757–763
11. K. Matsugi, G. Sasaki, O. Yanagisawa, Y. Kumagai, and K. Fujii, Electrical Resistivity of Pb-Free Sn-Zn Alloys for an AC-Low Voltage Fuse Element, *Mater. Trans.*, 2007, **48**, p 1105–1112
12. R.M. Shalaby, Effect of Indium Content and Rapid Solidification on Microhardness and Micro-Creep of Sn-Zn Eutectic Lead Free Solder Alloy, *Cryst. Res. Technol.*, 2010, **45**, p 427–432
13. T. Gancarz, J. Pstrus, P. Fima, and S. Mosinska, Thermal Properties and Wetting Behavior of High Temperature Zn-Al-In Solders, *J. Mater. Eng. Perform.*, 2012, **21**, p 599–605
14. J. Glazer, Microstructure and Mechanical Properties of Pb-Free Solder Alloys for Low-Cost Electronic Assembly, A review, *J. Electron. Mater.*, 1994, **23**, p 693–700
15. M. Kamal and E.S. Gouda, Effect of Zinc Additions on Structure and Properties of Sn-Ag Eutectic Lead-Free Solder Alloy, *J. Mater. Sci.: Mater. Electron.*, 2008, **19**, p 81–84
16. www.matweb.com. Accessed 20 August, 2013
17. S.G. Teodorescu, R.A. Overfelt, and S.I. Bakhtiyarov, An Inductive Technique for Electrical Conductivity Measurements on Molten Metals, *Int. J. Thermophys.*, 2001, **22**, p 1521–1535
18. L.R. Garcia, W.R. Osório, L.C. Peixoto, and A. Garcia, Mechanical Properties of Sn-Zn Lead-Free Solder Alloys Based on the Microstructure Array, *Mater. Charact.*, 2010, **61**, p 212–220
19. S.W. Kim, J. Lee, B.M. Jeon, E. Jung, S.H. Lee, K.H. Kang, and K.T. Lim, Thermophysical Properties of Sn-Ag-Cu Based Pb-Free Solders, *Int. J. Thermophys.*, 2009, **30**, p 1234–1241
20. J. Jiang, J.-E. Lee, K.-S. Kim, and K. Suganuma, Oxidation Behavior of Sn-Zn Solders Under High-Temperature and High-Humidity Conditions, *J. Alloy. Compd.*, 2008, **462**, p 244–251
21. L. Garcia, W. Osorio, L. Peixoto, and A. Garcia, Wetting Behavior and Mechanical Properties of Sn-Zn and Sn-Pb Solder Alloys, *J. Electron. Mater.*, 2009, **38**, p 2405–2414
22. Y. Chan, M. Chiu, and T. Chaung, Intermetallic Compounds Formed During the Soldering Reactions of Eutectic Sn-9Zn with Cu and Ni Substrates, *Z. Metallkd.*, 2002, **93**, p 95–98
23. Y. Cui, X.J. Liu, I. Ohnuma, R. Kainuma, H. Ohtani, and K. Ishida, Thermodynamic Calculation of the In-Sn-Zn Ternary System, *J. Alloy. Compd.*, 2001, **320**, p 234–241
24. W.F. Gale and T.C. Totemair, Ed., *Smithells Metals Reference Book*, 8th ed., Elsevier, Amsterdam, 2004, p 14-1–14-3
25. T. Siewert, S. Liu, D.R. Smith, and J.C. Madeni, *Database for Solder Properties with Emphasis on New Lead-Free Solders*, National Institute of Science and Technology & Colorado School of Mines, Colorado, 2002